Available online at www.sciencedirect.com
ScienceDirect
Earth and Planetary Science Letters 256 (2007) 419–432
EPSL
www.elsevier.com/locate/epsl

High- and low-latitude orbital forcing of early hominin habitats in South Africa

Philip J. Hopley [a,b,*], Graham P. Weedon [c], Jim D. Marshall [a], Andy I.R. Herries [d,e], Alf G. Latham [b], Kevin L. Kuykendall [f]

[a] *Department of Earth and Ocean Sciences, University of Liverpool, Liverpool, L69 3GP, UK*
[b] *School of Archaeology, Classics and Egyptology, University of Liverpool, Liverpool, L69 3GS, UK*
[c] *Climate and Land-Surface Interaction Centre (CLASSIC), Department of Geography, School of Environment and Society, University of Wales Swansea, Swansea, SA2 8PP, UK*
[d] *School of Medical Sciences, University of New South Wales, 2052, Sydney, Australia*
[e] *Geomagnetism Laboratory, University of Liverpoool, L697ZE, UK*
[f] *Department of Archaeology and Prehistory, University of Sheffield, Sheffield, S1 4ET, UK*

Received 20 September 2005; received in revised form 18 January 2007; accepted 25 January 2007
Available online 3 February 2007
Editor: H. Elderfield

Abstract

Reconstructions of African palaeoenvironments are essential for a full understanding of early hominin evolution, but they are often hampered by low-resolution or discontinuous climatic data. Here we present high-resolution oxygen ($\delta^{18}O$) and carbon ($\delta^{13}C$) isotope time series for the Pliocene/early Pleistocene (1.99 to 1.52 Ma) of South Africa, derived from the Buffalo Cave flowstone deposit. The $\delta^{18}O$ data are dominated by variations at the orbital precession period (18–23 ka), as is typical for records of sub-tropical monsoon rainfall. The $\delta^{13}C$ data indicate the proportion of savannah grasses (C_4 plants) compared to trees and shrubs (C_3 plants), and this signal is dominated by an obliquity periodicity (40 ka), commonly associated with high-latitude ice-sheet dynamics. A rapid increase in savannah grass proportions between 1.78 and 1.69 Ma coincides with a pulse in African mammal turnover, and lends support to an adaptive link between the appearance of African *Homo erectus* and the increasingly savannah-dominated environment.

Keywords: stable isotopes; flowstone; South Africa; *Homo*; savannahs; precession

1. Introduction

Global cooling trends and Milankovitch periodicities are features of Late Neogene to Recent climate records that have been suggested to drive evolution of African mammalian faunas, including hominins [1–3]. Studies of hominin speciation, extinction and migration have focussed on either directional trends of global cooling [1,3] or on the magnitude and frequency of climatic variability [2] by referring to these elements within marine palaeoclimate records [4]. While there are sound theoretical and empirical reasons to link climatic change causally to hominin evolution [3], it has yet to

* Corresponding author. Present address: School of Geographical Sciences, University of Bristol, University Road, BS8 1SS, UK. Tel.: +44 117 9289111.
E-mail address: phil.hopley@bristol.ac.uk (P.J. Hopley).

0012-821X/$ - see front matter © 2007 Elsevier B.V. All rights reserved.
doi:10.1016/j.epsl.2007.01.031

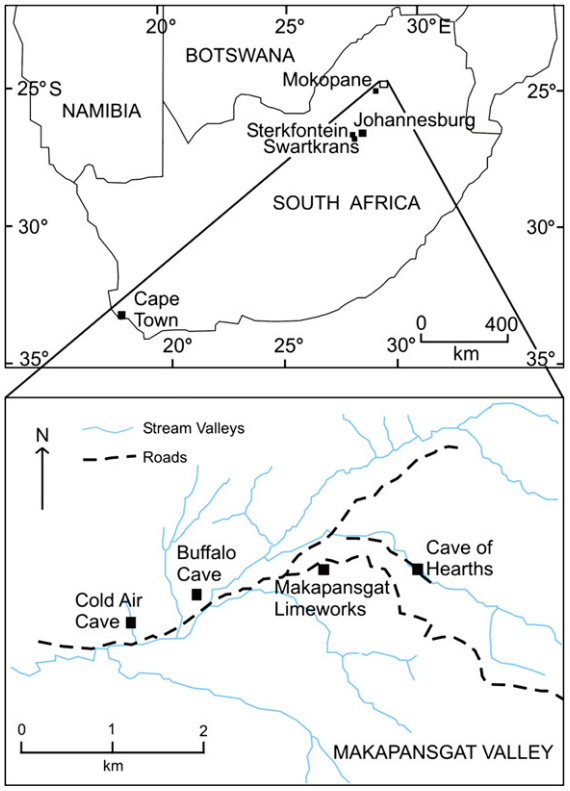

Fig. 1. Map of the Makapansgat Valley, Limpopo Province, north-eastern South Africa. The Buffalo Cave locality and other cave sites referred to in the text are marked.

be demonstrated that the Late Neogene marine record [4] is a faithful indicator of sub-tropical and tropical African terrestrial palaeoclimates. Existing long-term records of African climate change have been constructed using terrestrial components within marine sediment cores [1,5,6] and produce highly spatially-averaged proxy records. Local environmental records of hominin habitats are often limited by sparse and time-averaged faunal and sedimentary deposits [7–9].

Vegetation dynamics are widely regarded as the principal link between global climatic changes and faunal evolution in tropical ecosystems [1,3,9,10], and are therefore the key to interpreting trends in mammalian and hominin evolution. However, there is current uncertainty over the principal mechanisms that govern the distribution of the two dominant tropical floras — savannah (C_4) grassland and tropical forest (C_3). Changes in the proportion of C_4 and C_3 vegetation in a tropical ecosystem can either be controlled by high-latitude forcing of global temperature and atmospheric pCO_2 [11,12], or by local forcing of monsoon rainfall intensity [6,13]. This study uses carbon and oxygen isotope time series from a 2.4 m thick flowstone (cave carbonate deposit) to investigate the relationship between orbital forcing, vegetation change, and monsoon rainfall. The flowstone was collected from Buffalo Cave (24° 08′ S, 29° 11′ E) in the Makapansgat Valley (Fig. 1), Limpopo Province, South Africa. Buffalo Cave (BC) has yielded an Early Pleistocene fauna [14] and is situated 1.5 km to the west of the Plio-Pleistocene hominin-bearing Makapansgat Limeworks site (Fig. 1).

2. Methods

2.1. Stratigraphy and palaeomagnetism

The northern section of the Buffalo Cave deposits are exposed in three mined areas, informally known as the Lower Cave, the Shelf and the Upper Cave [14,15]. The BC flowstone is exposed in the Lower Cave and represents a second phase of speleothem deposition within the overall sedimentary sequence. The 2.4 m flowstone was laid down continually except at a depth of 14.09 m where a probable hiatus is marked by a thin layer of fossil bat guano (Fig. 2). Overlying the BC flowstone is a series of consolidated red muds and breccias, and overlying this is a series of coarser-grained deposits containing large quantities of fossil bone fragments. This in turn is overlain by more localised speleothem deposits, red muds and bone breccias (Fig. 2).

The overlying fossil-bearing deposits and the BC flowstone have been dated by combining evidence from biostratigraphy and palaeomagnetic polarity measurements (Fig. 2). The mammal assemblages from the Upper Cave and Shelf deposits are dated to between 0.6 and 0.96 Ma, based on faunal correlation with radiometrically-dated east African counterparts [15]. The faunal deposits all have a reversed direction of polarity that can be placed within the Matuyama magnetochron of the Global Polarity Timescale, between the end of the Jaramillo normal event at 0.99 Ma and the Bruhnes–Matuyama boundary at 0.78 Ma (Fig. 2). The underlying sediments have intermediate and normal directions of polarity that correspond to the Jaramillo event between 1.07 and 0.99 Ma. Oriented samples taken from between 13.1 m and 13.7 m depth, including the top section of the BC flowstone, have reversed directions of magnetization that places them in the Matuyama magnetochron between 1.77 and 1.07 Ma (Fig. 2). The majority of the underlying flowstone contains few detrital inclusions such that no stable magnetization is recorded. Three samples from the base of the BC flowstone record one normal and two intermediate normal directions, which are likely to correspond with the Olduvai event between 1.95 and

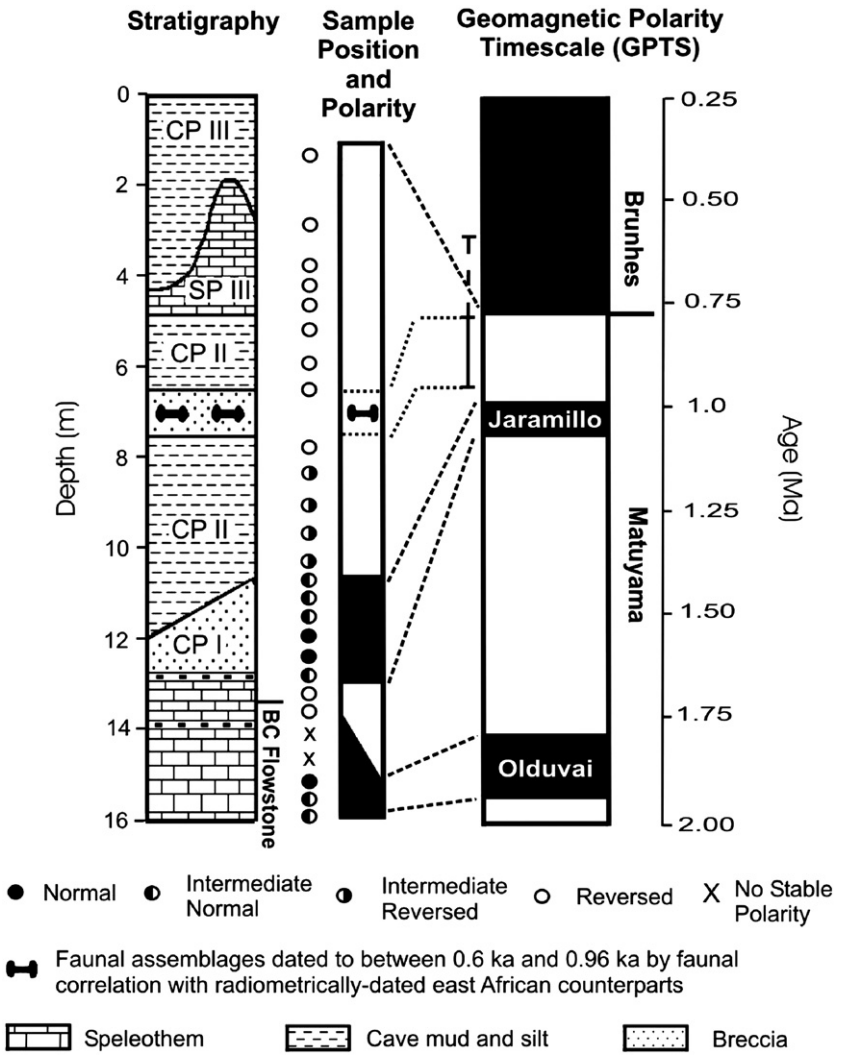

Fig. 2. Correlation of the Buffalo Cave magnetostratigraphy to the Geomagnetic Polarity Timescale (GPTS). The faunal assemblages from the Upper Cave and Shelf deposits (indicated using the bone symbol at the 7 m level), are dated to between 0.6 and 0.96 Ma, based on faunal correlation with radiometrically-dated east African counterparts [15]. These faunal deposits have a reversed direction of polarity, indicating that they belong in the Matuyama magnetochron of the Global Polarity Timescale. The combination of biostratigraphic and magnetostratigraphic evidence enables the age of the faunal deposits to be constrained to between 0.78 Ma (the Bruhnes–Matuyama boundary) and 0.96 Ma (the maximum age on the basis of biostratigraphy). Further magnetostratigraphic evidence enables the non-fossiliferous deposits of the Buffalo Cave sedimentary sequence to be placed within the GPTS. Clastic (CP) and Speleothem (SP) Phases are indicated on the sedimentary sequence. The stable isotope measurements shown in Figs. 4–7 were taken from the B.C. flowstone between the depths of 16.1 m and 13.7 m.

1.78 Ma (Fig. 2). Using the faunally constrained polarity record, it can be inferred that the BC flowstone accumulated some time between 1.07 and 1.95 Ma (Figs. 2 and 3). Orbital tuning was then used to further constrain the age of the BC flowstone.

2.2. Stable isotopes

Continuous sampling for stable isotope analysis at 5 mm intervals, using a diamond-tipped micro-drill with a diameter of 1.5 mm, yielded 483 samples. Standard methods were used to measure $\delta^{18}O$ and $\delta^{13}C$ on a VG SIRA mass spectrometer using an ISOCARB autopreparation device at the University of Liverpool. Long-term laboratory reproducibility is better than 0.1‰ for both isotope ratios.

The Buffalo Cave flowstone also contained acid insoluble organic matter (e.g. humic acids) that was extracted by centrifugation, following dissolution of 5–15 g of flowstone (approximately 1 cm in vertical

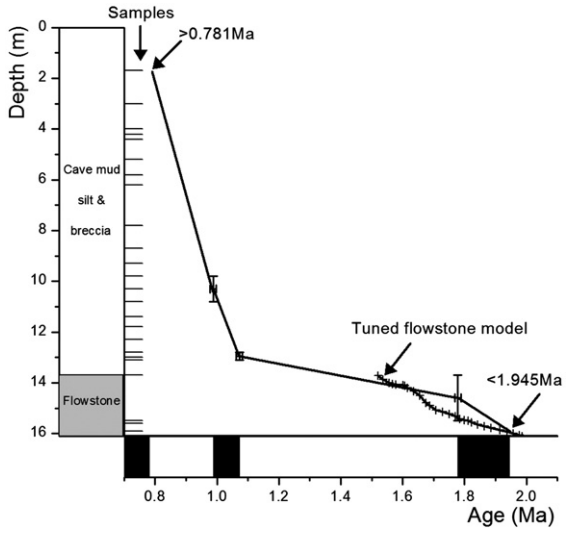

Fig. 3. Age–Depth plot of the Buffalo Cave sedimentary sequence and palaeomagnetic samples and age constraints. The age model of the orbitally-tuned Buffalo Cave flowstone, as used in Figs. 5–7, is also illustrated.

thickness) in 2 M HCl. Carbon isotope composition was determined for 26 samples of organic matter within the flowstone by combusting the freeze-dried humic fraction with Cu(II)O and silver wire in quartz tubes at 850 °C for 2 h prior to isotopic analysis. The resultant CO_2 was separated cryogenically and carbon isotope ratios were measured at the University of Liverpool. Accuracy and reproducibility were determined by replicate analysis of USGS 24 graphite standard and an internal humic acid standard. Long-term reproducibility (σ) is ±0.25‰.

For trace element analysis, aliquots of approximately 5 mg of powdered flowstone were dissolved in dilute nitric acid and analysed for Ca, Mg and Sr on a Perkin Elmer Optima 3300RL ICP-AES at Royal Holloway, University of London. Analytical precision was determined using an internal speleothem standard. Reproducibility (2σ) of Mg/Ca molar ratios is ±0.00065.

3. Results

3.1. Trace elements and carbon isotopes

The Mg/Ca ratio in speleothems varies in response to changes in the dissolution of the carbonate host-rock and to changes in speleothem precipitation. A positive correlation between speleothem $\delta^{13}C$ and the Mg/Ca ratio can indicate that precipitation effects (e.g. prior calcite precipitation) are controlling the variation of both parameters [16]. However, the negative correlation between $\delta^{13}C$ and the Mg/Ca ratios observed in the Buffalo Cave flowstone (Fig. 4) indicates that precipitation effects had minimal influence over the measured Mg/Ca ratios. Instead, its likely that the observed variation in Mg/Ca ratios reflect climatic or vegetation change through changes in the partial pressure of soil CO_2, resulting in more acidic percolating waters and a greater degree of host-rock dissolution [16]. In this scenario, the low $\delta^{13}C$ values of forested C_3 vegetation correlates with increased Mg/Ca ratios, as observed in the BC flowstone (Fig. 4).

Carbon isotopes in soil-derived carbonate and organic deposits can be used as a tracer of C_3 and C_4 vegetation because the two plant types have markedly different carbon isotope compositions of about −26‰ and −13‰ respectively [12,17]. The $\delta^{13}C$ values of the humic fraction of organic matter preserved within the BC flowstone calcite were used as a first indication of palaeovegetation. The humic acid $\delta^{13}C$ values range from −27.3‰ to −21.1‰ with a mean value of −23.7‰ (see Appendix A). After correction for the −1.2‰ isotopic fractionation between humic acids and bulk soil organic matter [18], the measured organic $\delta^{13}C$ values were converted to a percentage of C_4 grasses using the values for C_3 plants and C_4 grasses quoted above. This calculation indicates that palaeovegetation varied from 0% to 47% C_4 grasses, with a mean of 27% C_4 grasses. This reconstruction is consistent with the mixed savannah–woodland, composed of both C_3 and C_4 vegetation, that is present in northern South Africa in both the modern day and in the Plio-Pleistocene [7,8].

Carbon isotopes in speleothem carbonate can be used as a palaeovegetation proxy, provided that the isotopic signal transferred via soil CO_2 can be distinguished from the carbon component sourced from dissolution of the carbonate host-rock [19]. This method has the potential of providing a far higher resolution palaeovegetation record than that derived from humic acid $\delta^{13}C$. We assume that the carbonate palaeovegetation signal has been diluted with a typical host-rock proportion of 15±5% e.g. [20,21] and that the host-rock has a mean $\delta^{13}C$ value of −0.9‰ ($\delta^{13}C$ value for Precambrian dolomites in the Makapansgat Valley [22]). Following published methodology [21] this produces end-member speleothem carbonate $\delta^{13}C$ values of −8.0‰ for a 100% C_3 vegetation and +1.3‰ for 100% C_4 vegetation. Using these end-members, the range of measured $\delta^{13}C$ carbonate values for the BC flowstone (−8.2‰ to −2.6‰; see Appendix B) convert to values for the percentage of C_4 plant cover, ranging from 0% to 67%, with an uncertainty of approximately 10% (Fig. 6). The lower half of the BC carbonate record (16.11 m to 14.995 m) has significantly lower $\delta^{13}C$ values

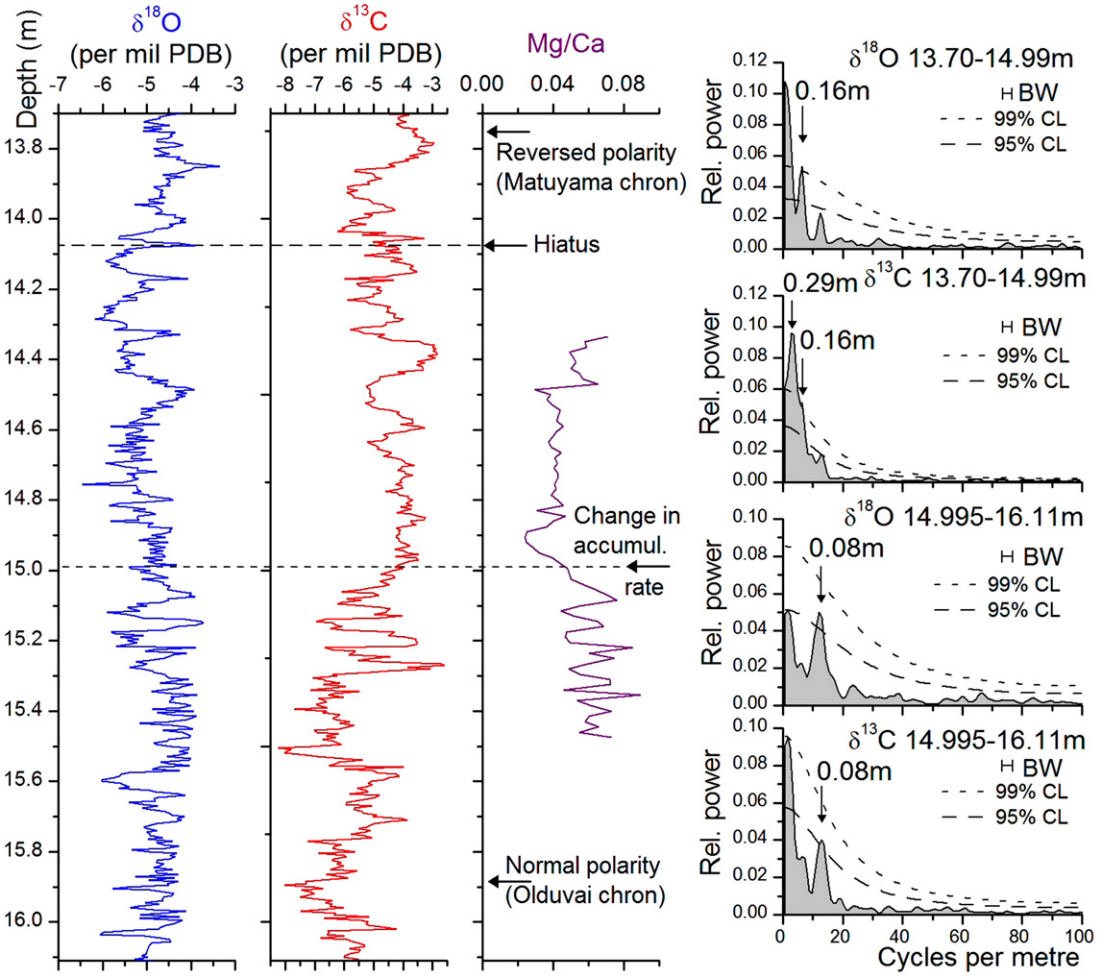

Fig. 4. Spectral analyses of Buffalo Cave flowstone $\delta^{18}O$ and $\delta^{13}C$ depth records. The cycle wavelength changes at a depth of 14.99 m indicating a change in growth rate above and below this datum. The statistically significant spectral peaks indicate cycles with wavelengths of 0.29 m, 0.16 m and 0.08 m. The presence of more than six 0.16 m and 0.08 m cycle repetitions plus the significant spectral peaks indicates regular cyclicity at these wavelengths [80]. Reduction in Mg/Ca ratio at a depth of 14.99 m coincides with an increase in $\delta^{13}C$. The lower arrow indicates the position of the normal intermediate palaeomagnetism sample (depth of 15.85 to 15.89 m) assigned to the Olduvai event (1.79–1.95 Ma). BW = bandwidth; CL = confidence level.

(mean = −5.7‰, S.D. = 1.0‰) than the upper half of the record (14.99 m to 13.7 m; mean = −4.4‰, S.D. = 0.75‰). A relatively rapid increase in average carbon isotope values between 15.30 m and 14.99 m is interpreted to reflect an increase in the mean proportion of C_4 grasses (Figs. 4 and 6).

3.2. Oxygen isotopes

The oxygen isotopic composition of speleothems is the end-product of a number of different processes within the atmosphere and karst zone including changes in temperature, rainfall source, rainfall amount and calcite precipitation effects [23]. A detailed understanding of oxygen isotope variability in the present day and recent past is important to aid the interpretation of speleothem $\delta^{18}O$ time series in a specific karst region. Interpretation of the oxygen isotope records presented in this study is aided by the measurements of oxygen isotopes in precipitation from Pretoria [24], groundwaters from the summer rainfall zone of Southern Africa [25–27] and the Holocene and Late Pleistocene stalagmite records from Cold Air Cave (see Fig. 1), also in the Makapansgat Valley [27].

Information on the variation of the oxygen isotope composition of rainfall over glacial–interglacial timescales has been extracted from groundwater sources in South Africa and shows that $\delta^{18}O$ of rainfall was

approximately −5‰ during the last glacial period and −4‰ during the Holocene [25–27]. Once the reduction in global ice volume has been taken into account (equivalent to an ~1.3‰ reduction in the oxygen isotope composition of ocean water), it is evident that there was approximately a 2.3‰ increase in the $\delta^{18}O$ composition of South African rainfall in response to the 5 °C to 6 °C of warming that occurred between the last glacial period and the Holocene [25–27]. This 0.3–0.4‰ per °C relationship between temperature and the $\delta^{18}O$ composition of rainfall in Southern Africa lies within the range quoted for sub-tropical regions across the globe [28,29]. However, there is an independent and opposite temperature effect that occurs during the precipitation of speleothem calcite (−0.25‰ per °C [30]) that is responsible for a decrease in calcite $\delta^{18}O$ of approximately 1‰ during the transition from the last glacial period into the Holocene. This essentially cancels out the effect of temperature on the $\delta^{18}O$ composition of rainfall, leaving the global ice-volume effect as the dominant control on speleothem $\delta^{18}O$. The 1–2‰ change from glacial to interglacial oceans [4,31] successfully explains the 1‰ decrease in $\delta^{18}O$ observed during the transition from the last glacial period to the Holocene in the Cold Air Cave (see Fig. 1) T8 stalagmite [27].

It is reasonable to assume that earlier glacial–interglacial cycles in the Plio-Pleistocene speleothems from South Africa were also dominated by ice-volume effects, as the opposite signs of the calcite $\delta^{18}O$ and the rainfall $\delta^{18}O$ palaeotemperature effects would have continued to largely cancel each other out. The mean $\delta^{18}O$ value of the BC flowstone of −4.9‰ (ranging from −6.5‰ to −3.4‰; see supplementary data in the Appendix) is approximately 1‰ lower than the equivalent value measured in the Holocene T8 stalagmite [27] from nearby Cold Air Cave (the mean $\delta^{18}O$ value is approximately −4.0‰ after the values of the aragonitic speleothem have been converted to a calcite equivalent). It is apparent that smaller global ice volumes and lower $\delta^{18}O$ values of ocean water are at least partly responsible for the lower values of speleothem $\delta^{18}O$ in the Plio-Pleistocene of the Makapansgat Valley, relative to the Holocene speleothems [27]. The variability of the ice-volume effect at and around the Pliocene/Pleistocene boundary was less than 1‰ ([4,31]; see Fig. 7), indicating that ice-volume effects alone are not sufficient to explain the 1 to 2‰ variability of the $\delta^{18}O$ record from Buffalo Cave (see Figs. 6 and 7). The remaining $\delta^{18}O$ variability must be explained by changes in the isotopic composition of rainfall.

There is currently little data to shed light on the pre-Holocene variability of rainfall $\delta^{18}O$ over southern Africa, especially at times when the magnitude of glacial–interglacial cycles was reduced. It is therefore useful to consider the controls on $\delta^{18}O$ in rainfall over the entire eastern African monsoon region and its Indian Ocean source. It has been demonstrated that there is a strong link between the $\delta^{18}O$ composition of rainfall over eastern and southern Africa and the interannual variability of circulation in the Indian Ocean [32], known as the Indian Ocean Dipole (IOD). The anomalous years of the IOD are characterised by a reversal in the sign of the sea surface temperature (SST) gradient (from east to west) and change in the direction of surface zonal winds from westerlies to easterlies across the ocean basin [33]. Associated with the anomalously warm SSTs in the western Indian Ocean is an increase in monsoon rainfall over tropical east Africa and a significant increase in the $\delta^{18}O$ of this rainfall [32]. These greater $\delta^{18}O$ values during the East African rainy seasons are related to anomalous upper-air convergence and low-level divergence over East Africa when vertical ascent and convective activity are subdued. Such conditions lead to reduced rainout and less intense distillation processes in convective clouds and thus greater $\delta^{18}O$ values over the western Indian Ocean and east Africa. Extremes in the IOD are associated with a difference in $\delta^{18}O$ of 5.3‰ in east Africa (Entebbe) during the months of October–December. During southern hemisphere precessional maxima, when the inter-tropical convergence zone (ITCZ) had migrated southward, the Makapansgat Valley of South Africa (24° S) would have received increased rainfall amounts with greater $\delta^{18}O$ values, as occurring in eastern Africa today [32]. During precessional minima, the northward expansion of the ITCZ and the equator-ward expansion of the westerlies and their associated weather disturbances would have brought cooler and dryer air from the Atlantic to north eastern South Africa [34,35]. With a large landmass to the south-west of the Makapansgat Valley, it is likely that the continental effect would have influenced rainfall $\delta^{18}O$ during these precessional minima, resulting in more negative $\delta^{18}O$ values. On the basis of these arguments, we suggest that the precessional cycle at Makapansgat was characterised by more positive $\delta^{18}O$ values during humid insolation maxima and more negative $\delta^{18}O$ values during dry insolation minima.

Therefore, the most likely interpretation of the Buffalo Cave flowstone $\delta^{18}O$ record is that it is predominantly a proxy of monsoon intensity, but it also contains a minor component of global ice-volume effects. Irrespective of the complexities of quantifying the BC $\delta^{18}O$ values in terms of global ice volume and monsoon intensity, it is evident that there is a strong and repeated climatic control on the $\delta^{18}O$ values of the flowstone.

4. Time-series analysis and orbital tuning

4.1. Methods

The data were detrended using a linear least-squares regression and spectral estimation used an algorithm for irregularly spaced data [36] with corrections for high-frequency bias applied using the method of Schulz and Mudelsee [37]. Orbital tuning of the data was based on magnetostratigraphic dating constraints (see Fig. 5) and on matching amplitude modulation of the filtered data with the amplitude modulation of the Pliocene/early Pleistocene precession index [38]. At 24° South the solar insolation history is almost identical to the precession history [38]. Tuning proceeded as though maximum $\delta^{18}O$ corresponds to maximum precession and maximum solar insolation, based on our interpretation of the late Pleistocene to Recent speleothem record from Cold Air Cave [27].

4.2. Results

Spectral analysis of the BC carbon and oxygen isotopic records was used to test for the presence of regular sedimentary cyclicity that can be diagnostic of orbital-climatic cyclicity [39]. The spectra indicate a change in the wavelength of the dominant oxygen isotope cyclicity from 0.08 m to 0.16 m at a depth of approximately 14.99 m (Fig. 4). The change in cycle wavelength is interpreted to record a change in accumulation rate, and this is coincident with an abrupt change in the colour, organic carbon content, Mg/Ca ratio and $\delta^{13}C$ of the flowstone carbonate (Fig. 4). In the top part of the record the 0.16 m and 0.29 m cycles (ratio 1.8) probably record obliquity and precession forcing respectively as the wavelength ratio of these cycles is not consistent with eccentricity and obliquity forcing (2.5). If the 0.08 m cycles in the lower interval (below the 14.99 m level) and the 0.16 m cycles in the upper interval record precession cycles, this implies 22 precession cycles in total or about 460 ka — consistent with the magnetostratigraphic age controls (see Fig. 5).

Band-pass filtering [40] of the BC flowstone $\delta^{18}O$ data was used to isolate the cycles associated with the shortest wavelength spectral peaks above and below the 14.99 m level (Fig. 5). The filtered data show strong amplitude modulations reminiscent of the orbital-precession index, permitting the orbital tuning (Fig. 5). The tuning indicates that the sampled flowstone dates from 1.990 to 1.517 Ma. Power spectra for the $\delta^{18}O$ and

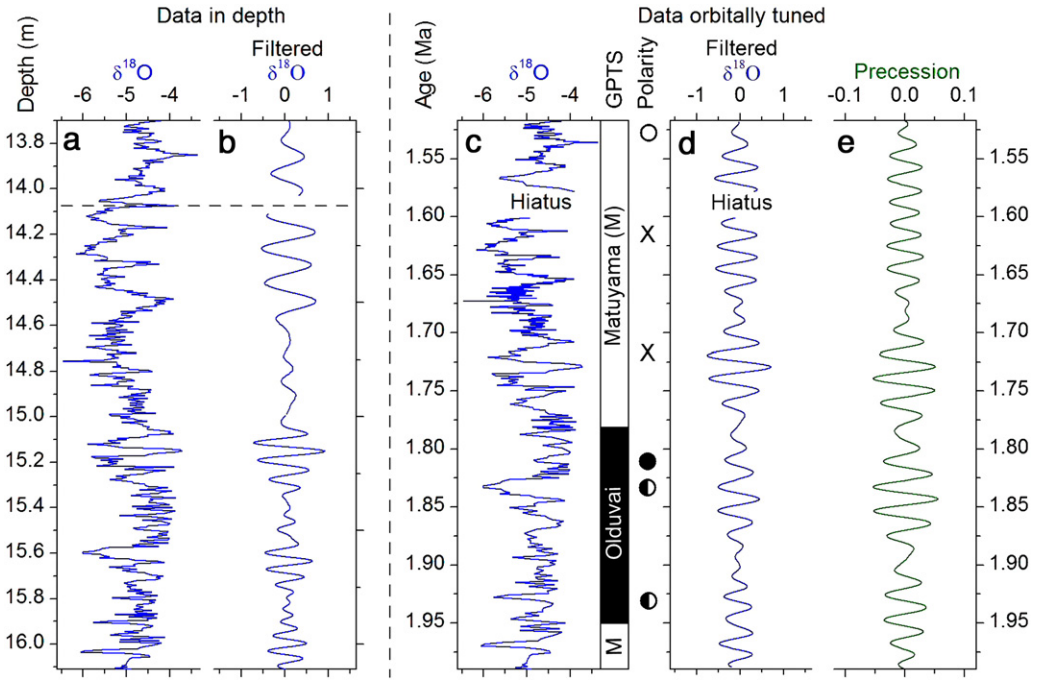

Fig. 5. Buffalo Cave flowstone $\delta^{18}O$ time series filtered and tuned to orbital precession [38]. (a) Buffalo Cave $\delta^{18}O$ record in depth (b) $\delta^{18}O$ time series filtered at central wavelengths of 16 cm (13.7–14.99 m) and 8 cm (14.995–16.11 m) (c) orbitally-tuned Buffalo Cave $\delta^{18}O$ time series (d) orbitally-tuned $\delta^{18}O$ time series filtered at precessional frequencies (19.4–22.8 ka) (e) orbital solution from 1.52 Ma to 1.98 Ma based on the orbital solution of Laskar et al. [38].

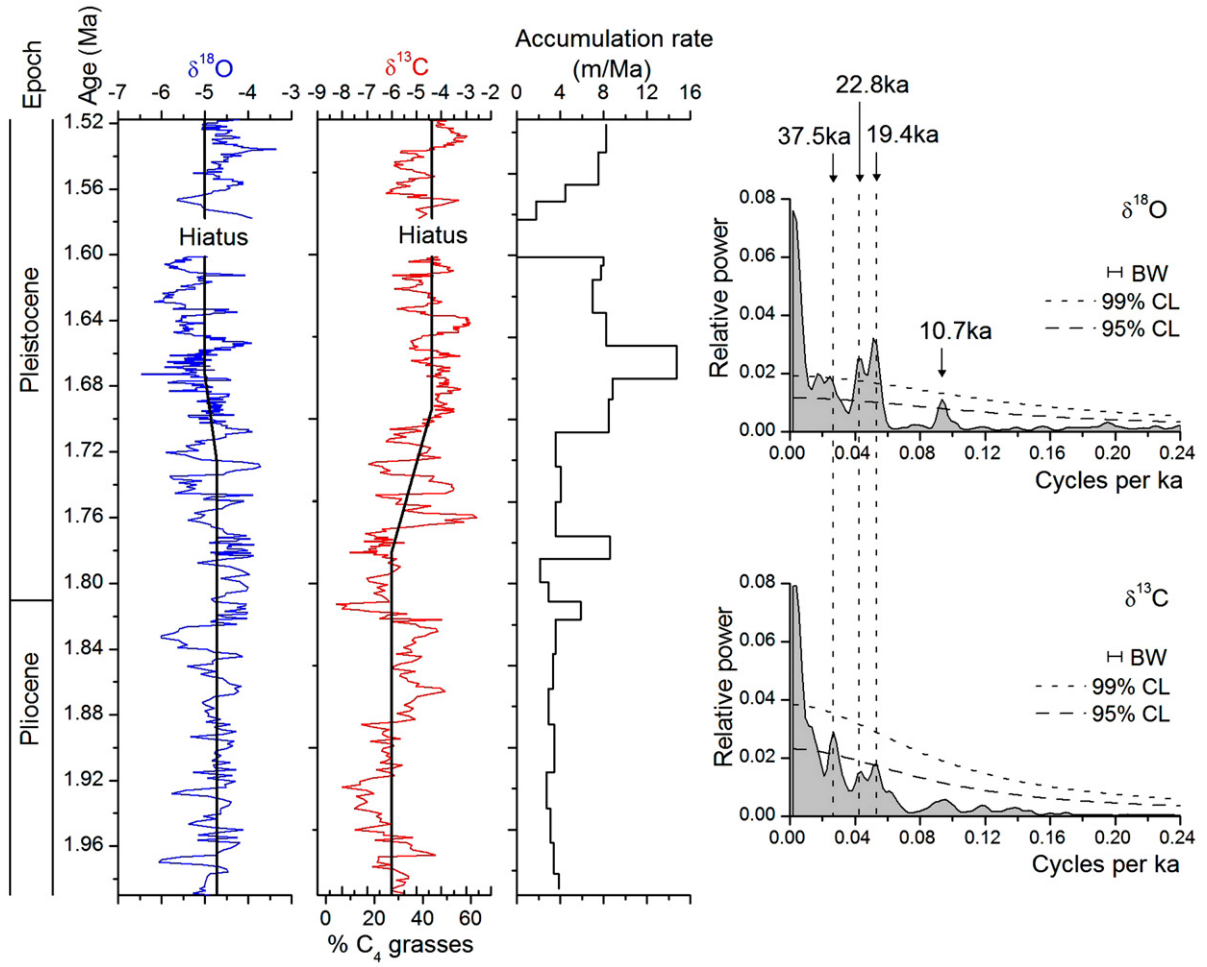

Fig. 6. Buffalo Cave flowstone $\delta^{18}O$ and $\delta^{13}C$ time series and associated spectra. The ca. 40 ka obliquity cycle is the dominant periodicity in the $\delta^{13}C$ record whereas the ca. 20 ka precessional cycles dominate the $\delta^{18}O$ record. The spectral peak for the $\delta^{18}O$ record labelled 10.7 ka represents the second harmonic of the precession cycles caused by non-sinusoidal oscillations. The % C_4 grasses values are determined using organic matter $\delta^{13}C$ values to correct for the host-rock carbon contribution to carbonate $\delta^{13}C$. The Buffalo Cave flowstone was formed in a mixed C_3 and C_4 plant environment in which the proportion of the two plant types was highly variable. The accumulation rate in m/Ma was determined from the orbital tuning. An inferred approximate doubling of accumulation rate occurs at 1.71 Ma, concurrent with an increase in mean % C_4 grasses. Thick lines on the $\delta^{18}O$ and $\delta^{13}C$ plots indicate the changing average values. BW = bandwidth; CL = confidence level.

$\delta^{13}C$ records from the flowstone carbonate have evidence for the same orbital cycles (Fig. 6). However, $\delta^{18}O$ was dominated by precession cycles (22.8 and 19.4 ka) whereas $\delta^{13}C$ was dominated by obliquity cycles (37.5–40.2 ka).

5. Discussion

5.1. Orbital forcing in the Plio-Pleistocene of South Africa

The Buffalo Cave $\delta^{18}O$ time series is dominated by the 19 ka and 23 ka precession signal, and also contains a minor 40 ka obliquity component (Fig. 6). Precessional forcing of monsoon intensity in sub-tropical terrestrial environments is both an observed and a modelled phenomenon [41–43]. Oxygen isotope records in late Pleistocene tropical speleothems provide clear evidence for the precessional forcing of monsoon rainfall [44]. These records provide evidence to confirm that tropical monsoons vary in response to the intensity of the summer (July) solar radiation, with a small phase lag relative to July insolation during the Late Quaternary [45]. There are a number of proxy records that demonstrate continued precessional forcing of tropical monsoons throughout the Late Neogene [6,46,47].

In contrast to the $\delta^{18}O$ record, the $\delta^{13}C$ time series of the Buffalo Cave flowstone is dominated by the obliquity cycle (40 ka), with the 23 ka and 19 ka precessional cycles occurring as minor components (Fig. 6). The obliquity cycle is known to force high latitude climates, as variation in insolation over the obliquity cycle is greatest at high latitudes [48,49]. For this reason, the obliquity cycle is rarely seen in low latitude climate proxies, except in the chemically mixed oceans where it is indicative of high-latitude ice-sheet dynamics [48]. Obliquity is the dominant periodicity in marine $\delta^{18}O$ variation during the late Pliocene and early Pleistocene [48,49], rather than the dominant eccentricity cycles observed in the late Pleistocene [4,31]. Although there are no high-resolution proxy records for atmospheric pCO_2 in the early Pleistocene, it is likely that the dominant periodicity of pCO_2 variation occurred at the obliquity frequency, as variations in atmospheric pCO_2 are thought to lead and drive marine $\delta^{18}O$ variations [50,51]. The presence of the obliquity cycle in the Buffalo Cave $\delta^{13}C$ time series suggests that the proportion of C_4 grasses may have been responding to changes in the atmospheric partial pressure of CO_2, in agreement with carbon isotope proxies from the Late Pleistocene [11,52,53] and the west African Plio-Pleistocene pollen record of Dupont and Leroy [5].

It is well known that an increase in the proportion of C_4 grasses in tropical ecosystems is controlled by either an increase in temperature, a decrease in atmospheric pCO_2, a reduction in precipitation, or a combination of these three factors [12,13,54]. It has been demonstrated in the Late Pleistocene that the reduced levels of atmospheric pCO_2 in glacial periods have a greater impact on vegetation than the corresponding reduction of tropical temperatures, resulting in a net increase in C_4 grasses during glacial periods [11,52,53,55]. Long records of Late Pleistocene vegetation change [11,53,56] are shown to closely resemble the corresponding records of atmospheric pCO_2 [50] and marine $\delta^{18}O$ [4,31] and are therefore dominated by the eccentricity cycle in the Late Pleistocene. A Pliocene and Early Pleistocene pollen record from marine sediments off the coast of west Africa [5] is dominated by an obliquity (41 ka) periodicity, the dominant orbital parameter within marine $\delta^{18}O$ records during these epochs [48,49].

In these records of Pliocene and Early Pleistocene tropical vegetation change it is clear that the proportion of C_4 grasses is responding to glacial–interglacial climatic change, but it is not always clear whether temperature, atmospheric pCO_2 or precipitation amount is responsible for the observed changes. Huang et al. [13] demonstrated that the influence of atmospheric pCO_2 on tropical vegetation can be enhanced or reduced by local changes in precipitation amount during glacial–interglacial cycles. Schefuβ et al. [6] reached similar conclusions in their carbon isotope study in the Mid-Pleistocene of Southern Africa based on an Atlantic core from the Angola Basin. They demonstrated the importance of tropical Atlantic SST in controlling the percentage of C_4 grasses in Southern Africa at precessional frequencies, through its control over precipitation amount. Schefuβ et al. [6] argued that C_3 plants were favoured during the more humid periods over Southern Africa, which coincided with low SSTs in the tropical Atlantic.

The negative correlation between $\delta^{18}O$ and $\delta^{13}C$ in the Buffalo Cave flowstone at the precessional frequencies (see Fig. 6) provides further support for a link between the proportion of C_4 grasses and the amount of precipitation in Southern Africa. Sankaran et al. [57] demonstrate that the modern-day savannahs of tropical Africa are stable in regions that receive less than 650 mm of mean annual precipitation (MAP). Above this precipitation threshold, the savannah environment is unstable and heads towards the new equilibrium state of a closed canopy forest. Over the last 200 ka in Pretoria, mean annual precipitation has oscillated between 800 mm and 500 mm at the precessional frequencies [42], indicating that the threshold of 650 mm MAP [57] was routinely crossed in the late Pleistocene. This would have led to a repeated cycle in vegetation at the precessional frequencies in which drier conditions (lower $\delta^{18}O$ values) were associated with an increased percentage of savannah grasses (higher $\delta^{13}C$ values), as observed in the Buffalo Cave flowstone (see Fig. 6).

The Buffalo Cave flowstone demonstrates that independent orbital periodicities can dominate co-occurring monsoon rainfall and palaeovegetation proxies. This suggests that the rainfall signal is controlled by local variations in sub-tropical precessional forcing, whereas tropical vegetation is predominantly controlled by high-latitude variations in orbital obliquity, forced by variation in Early Pleistocene atmospheric pCO_2. The additional effect of monsoon rainfall on tropical vegetation is responsible for the coupling of the two parameters at the precessional frequency, especially when monsoon forcing is at its maximum (see Figs. 6 and 7).

5.2. Climatic change at 1.7 Ma

Evidence for tropical climate change at ca. 1.7 Ma has been obtained from ocean cores (onset of the Walker Circulation [58,59]) and African terrestrial deposits (increased aridity [1]). To test whether the arid climatic

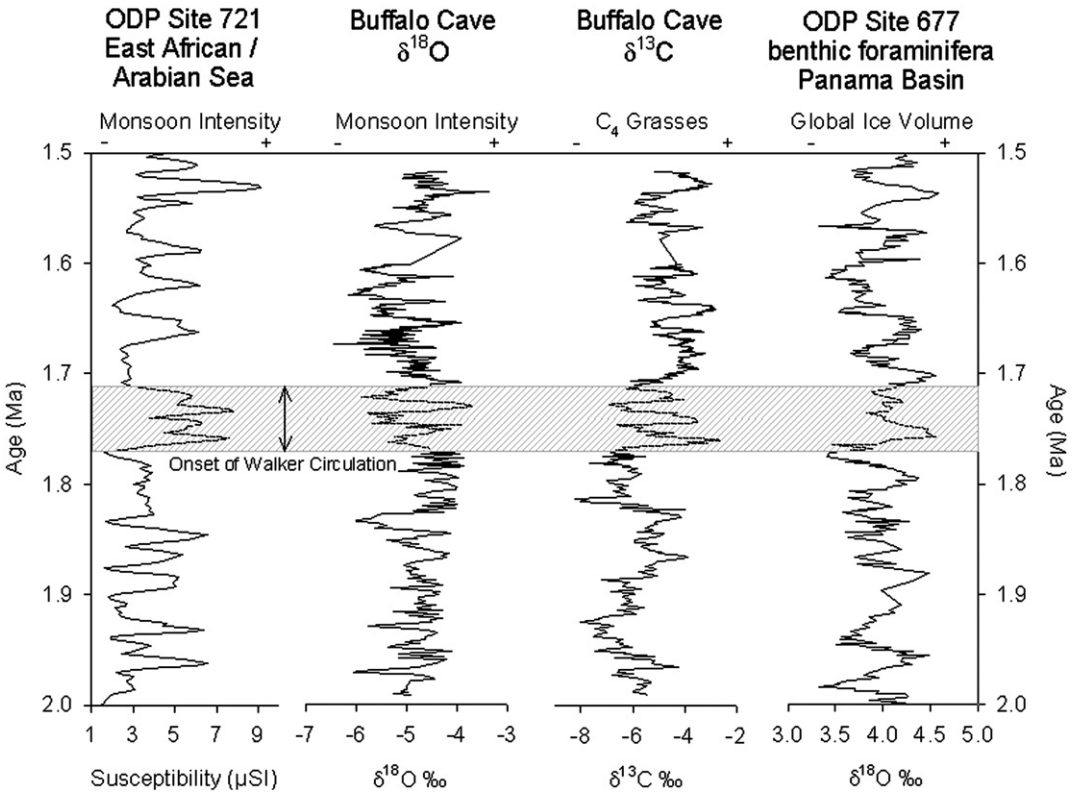

Fig. 7. Comparison of the Buffalo Cave flowstone $\delta^{18}O$ and $\delta^{13}C$ time series with global ice volume [4] and the intensity of the Indian Monsoon [46]. Shaded box indicates the onset of the Walker Circulation in the Pacific Ocean, as determined by [75].

event at 1.7 Ma is expressed in the Buffalo Cave flowstone, we used the RAMPFIT program [60] to investigate statistically significant shifts in the average values of the oxygen and carbon isotope records. Isotopic shifts between 1.8 Ma and 1.7 Ma are evident in both proxy records, the carbon isotopic shift being of greater magnitude than the oxygen (see Fig. 6). Following the interpretation of $\delta^{18}O$ as a proxy for monsoon rainfall (as discussed above), these isotopic shifts are interpreted as a reduction in precipitation and a corresponding increase in C_4 grasses (see Fig. 6). The shift in average $\delta^{13}C$, illustrated in Fig. 6 with the thick line, corresponds to an average palaeovegetation estimate of 27% C_4 plants before 1.78 Ma and 43% C_4 plants after 1.69 Ma. The combined rainfall and vegetation proxies derived from the Buffalo Cave flowstone lend strong support to the hypothesis that the restructuring of the tropical climate system at this time [58] led to greater aridity and increased savannah grassland over large areas of eastern and southern Africa.

Two major episodes of climate restructuring are evident in records of sub-tropical cooling towards the end of the Pliocene warm period. The first episode (between 3.0 and 2.5 Ma) was coincident with the onset of significant Northern Hemispheric Glaciation (NHG). The second episode (between 2.0 and 1.5 Ma) occurred, however, well after the onset of significant NHG [58]. High-latitude climate between 2.0 and 1.5 Ma was relatively stable, with no significant increase in global ice-volume occurring during this time (see $\delta^{18}O$ of benthic forams from ODP 677 [4]; plotted in Fig. 7). With a relatively stable ice-volume, the likelihood of ice-albedo effects influencing tropical climate during this episode is small. Instead, it has been suggested that the changes in tropical climate observed at ca. 1.7 Ma were related to the onset and intensification of the Walker Circulation (the east–west temperature gradient present in modern-day tropical Pacific surface-waters). There is evidence that in the mid-Pliocene, prior to the onset of the Walker Circulation, tropical and extra-tropical conditions resembled a permanent El Niño-like state [69]: the Pacific thermocline was deep, and the west–east SST gradient was greatly reduced compared with modern normal conditions [58–62]. It is clear that eastern Africa experienced increased aridity after the onset of the Pacific Walker circulation at 1.7 Ma (e.g.

[9,63]), and it is likely that these two events are related through global teleconnections.

The intensity of South African summer rainfall is predominantly controlled by SST anomalies in the south-western Indian Ocean, which are related to both the mode of the Indian Ocean Dipole [32,33] and to the strength of the El Niño Southern Oscillation (ENSO) in the Pacific Ocean [64,65]. Although there are years when the IOD anomalies coincide with ENSO anomalies in the Pacific Ocean, the two phenomena are considered to be independent from each other [33]. The link between South African rainfall and Pacific Ocean SST anomalies is exemplified by the fact that over the last 100 yr, 8 of the 12 drought years in the summer rainfall zone of South Africa took place during El Niño years [65]. This is because El Niño events, with warmer SST over the southern oceans, lead to a climatic bipolar pattern between continental southern Africa and the western Indian Ocean, which is characterised by reduced rainfall and deep convection over the subcontinent [64–66]. Global teleconnections between the tropical Pacific and the Indian Ocean can explain the links between the Walker Circulation, the Indian monsoon and African aridity in the modern day [64,67] and in the Pleistocene [63,68].

Evidence for the vegetation response to African aridity at 1.7 Ma is largely derived from carbon isotope and faunal evidence for a shift in vegetation composition towards a more savannah-dominated environment. At Sterkfontein, 200 km to the south of Buffalo Cave, a similar shift in C_4 grass biomass proportions has been recorded, as implied by an increase in the proportion of grazers within the fauna from 20% at 1.8 Ma to 68% at 1.7 Ma [69]. In equatorial Africa, a vegetational shift dating from 1.8–1.6 Ma has also been recorded [1,9,70–73] and has been linked to a period of faunal turnover [1,3] that is characterised by an increased proportion of savannah-adapted species [3,74]. In Kenya, soil carbonate $\delta^{13}C$ shows a pronounced increase in mean savannah grass proportions from 1.9 to 1.75 Ma [9]. These observations indicate a pan-African shift in the composition of vegetation in the Early Pleistocene, between 1.8 and 1.7 Ma.

Based on the evidence from the Buffalo Cave flowstone, we propose that southern Africa experienced a sudden reduction in rainfall at ca. 1.7 Ma, coincident with that observed in eastern Africa [63]. The rainfall regimes of eastern and southern Africa would have been linked through the behaviour of the IOD, especially at precessional maxima when the ITCZ was farther south. It is apparent that the permanent El-Niño conditions of the late Pliocene [75] resulted in wetter conditions over eastern and southern Africa relative to today; this was either a direct causal relationship, or it was mediated through the IOD. Onset of the Walker Circulation at 1.7 Ma [58,75] led to a reduction in African rainfall and an increase in arid-adapted vegetation (C_4 grasses) across Southern and Eastern Africa ([9,63,72]; see Figs. 6 and 7). This large-scale restructuring of floral communities inevitably led to a period of faunal turnover [1,3] and an increase in the number of savannah-adapted mammal species [3,74].

5.3. Climatic variability and early hominin habitats in South Africa

Previous studies have assumed that the South African faunal deposits were formed under constant ecological conditions, and consequently the palaeoenvironment has been interpreted as a highly mixed composite of forest, grasslands and wetlands [8,69,76]. While the present study indicates a mixed environment during the Plio-Pleistocene, it also highlights the rapidity with which the environment oscillated between forest-dominated and grass-dominated end-members. Faunal deposits rarely have temporal resolutions better than 100 ka [8,69,76], which indicates that most Plio-Pleistocene African faunal deposits are likely to be time-averaged amalgamations derived from both forest-dominated and grass-dominated environmental end-members. Because the BC flowstone time series is at a much greater temporal resolution than the coeval macro-faunal evidence, it is not known to what degree the precession and obliquity scale climatic forcing were responsible, separately or together, for the speciation and extinction events within the local mammalian communities.

In addition to evidence for mammalian turnover in Africa between 1.8 Ma and 1.7 Ma, the evolution of African *Homo erectus* must also be considered within the context of increasing savannah grass proportions. It has been suggested that *H. erectus* was the first hominin to develop a savannah-adapted morphology [77], as indicated by the similarity of its body shape and limb bone proportions to those of modern people living in tropical savannah grasslands. The first occurrence of *H. erectus* in East Africa is at ca. 1.7 Ma [78] based on specimens from Koobi Fora, Kenya, and the earliest record in South Africa is at ca. 1.7–1.4 Ma from Sterkfontein [79]. Both dates coincide with the increase of savannah grasslands across eastern and southern Africa, as discussed in this study, which we attribute to the onset of the Walker Circulation and increased African aridity at this time. While it is currently speculative to invoke climatic forcing of events in the hominin fossil record, it is apparent that there is both a temporal

correlation and a plausible mechanism to link the evolution of *H. erectus* in Africa with the restructuring of tropical climate and the spread of savannah grasslands.

6. Conclusions

This study has developed a high-resolution 2.0–1.5 Ma record of continuous climatic and vegetation change in South Africa from a late Pliocene to early Pleistocene flowstone. The dominant orbital parameter differs between the vegetation and climate proxy records — vegetation is responding to the obliquity forcing of global climate, whereas the monsoon rainfall signal is responding to low latitude precessional variation in Indian Ocean sea surface temperature and rainfall intensity. There is also a coupling of vegetation change to monsoon rainfall variability at the precessional frequency as C_4 grasses expanded during arid phases.

A rapid increase in the average percentage of C_4 grasses is observed at about 1.7 Ma (see Fig. 6), in agreement with other proxy records from eastern Africa. The increase in C_4 grasses at 1.7 Ma is related to the reorganisation of tropical climate at this time, specifically the onset of the Walker Circulation [58,75], which led to drier conditions over eastern and southern Africa. This event saw the restructuring of terrestrial ecosystems, an increase in faunal turnover, and the evolution of arid-adapted species [3,70] including early *Homo*.

Acknowledgements

This work was supported by a Natural Environment Research Council (UK) studentship (NER/A/2000/04058) awarded to PJH and the South African Heritage Resource Agency who issued the permit to sample from Buffalo Cave. Thanks to Steve Crowley and Jim Ball and Jacqui Duffett (NERC ICP-AES facility) for their technical support during the stable isotope and trace element measurements. We would also like to thank Thure Cerling, Julia Lee-Thorp and Mark Maslin for their insightful reviews of the manuscript.

Appendix A. Supplementary data

Supplementary data associated with this article can be found, in the online version, at doi:10.1016/j.epsl.2007.01.031.

References

[1] P.B. deMenocal, African climate change and faunal evolution during the Pliocene–Pleistocene, Earth Planet. Sci. Lett. 220 (2004) 3–24.
[2] R. Potts, Evolution and climate variability, Science 273 (1996) 922–923.
[3] E.S. Vrba, The fossil record of African antelopes (Mammalia, Bovidae) in relation to human evolution and paleoclimate, in: E.S. Vrba, G.H. Denton, T.C. Partridge, L.H. Burckle (Eds.), On the Connections Between Paleoclimate and Evolution, Yale University Press, New Haven, 1995, pp. 385–424.
[4] N.J. Shackleton, A. Berger, W.R. Peltier, An alternative astronomical calibration of the lower Pleistocene timescale based on ODP Site 677, Trans. R. Soc. Edinb. Earth Sci. 81 (1990) 251–261.
[5] L.M. Dupont, S.A.G. Leroy, Steps toward drier climatic conditions in Northwestern Africa during the Upper Pliocene, in: E.S. Vrba, G.H. Denton, T.C. Partridge, L.H. Burckle (Eds.), Paleoclimate and Evolution with Emphasis on Human Origins, Yale University Press, New Haven, 1995, pp. 289–298.
[6] E. Schefuβ, S. Schouten, J.H.F. Jansen, J.S. Sinninghe Damste, African vegetation controlled by tropical sea surface temperatures in the mid-Pleistocene period, Nature 422 (2003) 418–421.
[7] J.A. Lee-Thorp, A.S. Talma, Stable light isotopes and environments in the southern African Quaternary and Late Pliocene, in: T.C. Partridge, R.R. Maud (Eds.), The Cenozoic of Southern Africa, Oxford Monographs on Geology and Geophysics, Oxford University Press, Oxford, 2000, pp. 236–251.
[8] M. Sponheimer, K.E. Reed, J.A. Lee-Thorp, Combining isotopic and ecomorphological data to refine bovid paleodietary reconstruction: a case study from the Makapansgat Limeworks hominin locality, J. Hum. Evol. 36 (1999) 705–718.
[9] J.G. Wynn, Influence of Plio-Pleistocene aridification on human evolution: evidence from paleosols of the Turkana Basin, Kenya, Am. J. Phys. Anthropol. 123 (2004) 106–118.
[10] S. Cowling, M.A. Maslin, M. Sykes, Paleovegetation simulations of lowland Amazonia and implications for Neotropical allopatry and speciation, Quat. Res. 55 (2001) 140–149.
[11] A. Boom, R. Marchant, H. Hooghiemstra, J.S. Sinninghe Damsté, CO_2- and temperature-controlled altitudinal shifts of C_4- and C_3-dominated grasslands allow reconstruction of palaeoatmospheric pCO_2, Palaeogeogr. Palaeoclimatol. Palaeoecol. 177 (2002) 151–168.
[12] J.R. Ehleringer, T.E. Cerling, B.R. Helliker, C_4 photosynthesis, atmospheric CO_2 and climate, Oecologia 112 (1997) 285–299.
[13] Y. Huang, F.A. Street-Perrott, S.E. Metcalfe, M. Brenner, M. Moreland, K.H. Freeman, Climate change as the dominant control on glacial–interglacial variations in C_3 and C_4 plant abundance, Science 293 (2001) 1647–1651.
[14] K.L. Kuykendall, C.A. Toich, J.K. McKee, Preliminary analysis of the fauna from Buffalo Cave, northern Transvaal, South Africa, Palaeontol. Afr. 32 (1995) 27–31.
[15] A.I.R. Herries, K. Reed, K.L. Kuykendall, A.G. Latham, Speleology and magnetobiostratigraphic chronology of the Buffalo Cave fossil site, Makapansgat, South Africa, Quat. Res. 66 (2006) 233–245.
[16] J.C. Hellstrom, M.T. McCulloch, Multi-proxy constraints on the climatic significance of trace element records from a New Zealand speleothem, Earth Planet. Sci. Lett. 179 (2000) 287–297.
[17] M.H. O'Leary, Carbon isotopes in photosynthesis, BioScience 38 (1988) 328–336.
[18] É. Lichtfouse, S. Dou, S. Houot, E. Barriuso, Isotope evidence for soil organic carbon pools with distinct turnover rates — II. Humic substances, Org. Geochem. 23 (1995) 845–847.
[19] T.B. Coplen, I.J. Winograd, J.M. Landwehr, A.C. Riggs, 500,000-year stable carbon isotopic record from Devils Hole, Nevada, Science 263 (1994) 361–365.

[20] J.W. Beck, D.A. Richards, R.L. Edwards, B.W. Silverman, P.L. Smart, D.J. Donahue, S. Hererra-Osterheld, G.S. Burr, L. Calsoyas, A.J.T. Jull, D. Biddulph, Extremely large variations of atmospheric ^{14}C concentration during the last glacial period, Science 292 (2001) 2453–2458.

[21] D. Genty, A. Baker, M. Massault, C. Proctor, M. Gilmour, E. Pons-Branchu, B. Hamelin, Dead carbon in stalagmites: Carbonate bedrock paleodissolution vs. ageing of soil organic matter. Implications for ^{13}C variations in speleothems, Geochim. Cosmochim. Acta 65 (2001) 3443–3457.

[22] J. Veizer, R.N. Clayton, R.W. Hinton, Geochemistry of Precambrian carbonates: IV. Early Paleoproterozoic (2.25±0.25 Ga) seawater, Geochim. Cosmochim. Acta 56 (1992) 875–885.

[23] F. McDermott, Palaeo-climate reconstruction from stable isotope variations in speleothems: a review, Quat. Sci. Rev. 23 (2004) 901–918.

[24] IAEA/WMO, Global Network of Isotopes in Precipitation, the GNIP DatabaseAccessible at, http://isohis.iaea.org, 2006.

[25] T.H.E. Heaton, A.S. Talma, J.C. Vogel, Dissolved gas paleotemperatures and ^{18}O variations derived from Groundwater near Uitenhage, South Africa, Quat. Res. 25 (1986) 79–88.

[26] M. Stute, A.S. Talma, Glacial temperatures and moisture transport regimes reconstructed from noble gases and $\delta^{18}O$, Stampriet Aquifer, Namibia, Isotope Techniques in the Study of Environmental Change: Proceedings of an International Symposium on Isotope Techniques in the Study of Past and Current Environmental Changes in the Hydrosphere and the Atmosphere, IAEA, Vienna, 1997, pp. 307–318.

[27] K. Holmgren, J.A. Lee-Thorp, G.R.I. Cooper, K. Lundblad, T.C. Partridge, L. Scott, R. Sithaldeen, A.S. Talma, P.D. Tyson, Persistent millennial-scale climatic variability over the past 25,000 years in southern Africa, Quat. Sci. Rev. 22 (2003) 2311–2326.

[28] W. Dansgaard, Stable isotopes in precipitation, Tellus 16 (1964) 436–468.

[29] K. Rozanski, L. Araguas-Araguas, R. Gonfiantini, Relation between long-term trends of oxygen-18 isotope composition of precipitation and climate, Science 258 (1992) 981–985.

[30] H. Craig, The measurements of oxygen isotope palaeotemperature: stable isotopes in oceanographic studies and paleotemperatures, in: E. Tongiori (Ed.), Proceedings of the Third Spoleto Conference, Spoleto, Italy, Sischi and Figli, Pisa, 1965, pp. 161–182.

[31] N.J. Shackleton, J.P. Kennett, Late Cenozoic oxygen and carbon isotopic changes at DSDP site 284: implications for glacial history of the Northern Hemisphere and Antarctica, Init. Rep. Deep Sea Drill. Proj. 29 (1975) 801–807.

[32] M. Vuille, M. Werner, R.S. Bradley, R.Y. Chan, F. Keimig, Stable isotopes in East African precipitation record Indian Ocean zonal mode, Geophys. Res. Lett. 32 (2005) L21705, doi:10.1029/2005GL023876.

[33] N.H. Saji, B.N. Goswami, P.N. Vinayachandran, T. Yamagata, A dipole mode in the tropical Indian Ocean, Nature 401 (1999) 360–363.

[34] P.D. Tyson, Atmospheric circulation changes and palaeoclimates of southern Africa, S. Afr. J. Sci. 95 (1999) 194–201.

[35] M.J. Cockcroft, M.J. Wilkinson, P.D. Tyson, The application of a present-day climatic model to the late Quaternary in Southern Africa, Clim. Change 10 (1987) 161–181.

[36] W.H. Press, S.A. Teukolsky, W.T. Vetterling, B.P. Flannery, Numerical Recipes, the Art of Scientific Computing, Cambridge University Press, Cambridge, 1992 963 pp.

[37] M. Schulz, M. Mudelsee, REDFIT: estimating red-noise spectra directly from unevenly spaced paleoclimatic time series, Comput. Geosci. 28 (2002) 421–426.

[38] J. Laskar, P. Robutel, F. Joutel, M. Gastineau, A. Correia, B. Levrard, A long term numerical solution for the insolation quantities of the Earth, Astron. Astrophys. 428 (2004) 261–285.

[39] G.P. Weedon, The recognition and stratigraphic implications of orbital forcing of climate and sedimentary cycles, in: V.P. Wright (Ed.), Sedimentology Review, Blackwell, 1993, pp. 31–50.

[40] J.H. McClellan, T.W. Parks, L.R. Rabiner, A computer program for designing optimum FIR linear phase digital filters, IEEE Trans. Audio Electroacoust. 21 (1973) 506–526.

[41] E.M. Pokras, A.C. Mix, Earth's precession cycle and Quaternary climatic change in tropical Africa, Nature 326 (1987) 486–487.

[42] T.C. Partridge, P.B. deMenocal, S. Lorentz, M.J. Paiker, J.C. Vogel, Orbital forcing of climate over South Africa: a 200,000-year rainfall record from the Pretoria Saltpan, Quat. Sci. Rev. 16 (1997) 1125–1133.

[43] A.C. Clement, A. Hall, A.J. Broccoli, The importance of precessional signals in the tropical climate, Clim. Dyn. 22 (2004) 327–341.

[44] F.W. Cruz, S.J. Jr, I. Burns, W.D. Karmann, M. Sharp, A.O. Vuille, J.A. Cardoso, P.L. Ferrari, O. Silva Dias Jr., Insolation-driven changes in atmospheric circulation over the past 116,000 years in subtropical Brazil, Nature 434 (2005) 63–66.

[45] W.F. Ruddiman, What is the timing of orbital-scale monsoon changes? Quat. Sci. Rev. 25 (2006) 657–658.

[46] P.B. deMenocal, J. Bloemendal, Plio-Pleistocene climatic variability in subtropical Africa and the paleoenvironment of hominid evolution, in: E.S. Vrba, G.H. Denton, T.C. Partridge, L.H. Burckle (Eds.), Paleoclimate and Evolution with Emphasis on Human Origins, Yale University Press, New Haven, 1995, pp. 262–288.

[47] S.C. Clemens, D.W. Murray, W.L. Prell, Nonstationary Phase of the Plio-Pleistocene Asian Monsoon, Science 274 (1996) 943–948.

[48] W.F. Ruddiman, M.E. Raymo, A. McIntyre, Matuyama 41,000-year cycles: North Atlantic Ocean and northern hemisphere ice sheets, Earth Planet. Sci. Lett. 80 (1986) 117–129.

[49] M.E. Raymo, K. Nisancioglu, The 41 kyr world: Milankovitch's other unsolved mystery, Paleoceanography 18 (1–6) (2003) 1011.

[50] J.R. Petit, J. Jouzel, D. Raynaud, N.I. Barkov, J.-M. Barnola, I. Basile, M. Bender, J. Chappellaz, M. Davis, G. Delaygue, M. Delmotte, V.M. Kotlyakov, M. Legrand, V.Y. Lipenkov, C. Lorius, L. Pepin, C. Ritz, E. Saltzman, M. Stievenard, Climate and atmospheric history of the past 420,000 years from the Vostok ice core, Antarctica, Nature 399 (1999) 429–436.

[51] N.J. Shackleton, The 100,000-year ice-age cycle identified and found to lag temperature, carbon dioxide, and orbital eccentricity, Science 289 (2000) 1897–1902.

[52] G.J. Collatz, J.A. Berry, J.S. Clark, Effects of climate and atmospheric CO_2 partial pressure on the global distribution of C_4 grasses: present, past, and future, Oecologia 114 (1998) 441–454.

[53] A. Boom, G. Mora, A.M. Cleef, H. Hooghiemstra, High altitude C_4 grasslands in the northern Andes: relicts from glacial conditions? Rev. Palaeobot. Palynol. 115 (2001) 147–160.

[54] J.R. Ehleringer, R.K. Monson, Evolutionary and ecological aspects of photosynthetic pathway variation, Ann. Rev. Ecolog. Syst. 24 (1993) 411–439.

[55] S.A. Cowling, M.T. Sykes, Physiological significance of low atmospheric CO_2 for plant–climate interactions, Quat. Res. 52 (1999) 237–242.

[56] H. Hooghiemstra, Environmental and paleoclimatic evolution in Late Pliocene–Quaternary Colombia, in: E.S. Vrba, G.H. Denton, T.C. Partridge, L.H. Burckle (Eds.), Paleoclimate and Evolution with Emphasis on Human Origins, Yale University Press, New Haven, 1995, pp. 249–261.
[57] M. Sankaran, N.P. Hanan, R.J. Scholes, J. Ratnam, D.J. Augustine, B.S. Cade, J. Gignoux, S.I. Higgins, X. Le Roux, F. Ludwig, J. Ardo, F. Banyikwa, A. Bronn, G. Bucini, K.K. Caylor, M.B. Coughenour, A. Diouf, W. Ekaya, C.J. Feral, E.C. February, P.G.H. Frost, P. Hiernaux, H. Hrabar, K.L. Metzger, H. H.T. Prins, S. Ringrose, W. Sea, J. Tews, J. Worden, N. Zambatis, Determinants of woody cover in African savannas, Nature 438 (2005) 846–849.
[58] A.C. Ravelo, D.H. Andreasen, M. Lyle, A. Olivarez Lyle, M.W. Wara, Regional climate shifts caused by gradual global cooling in the Pliocene epoch, Nature 429 (2004) 263–267.
[59] P. Molnar, M.A. Cane, El Nino's tropical climate and teleconnections as a blueprint for pre-Ice Age climates, Paleoceanography 17 (2002) 1021.
[60] M. Mudelsee, Ramp function regression: a tool for quantifying climate transitions, Comput. Geosci. 26 (2000) 293–307.
[61] K.G. Cannariato, A.C. Ravelo, Pliocene–Pleistocene evolution of eastern tropical Pacific surface water circulation and thermocline depth, Paleoceanography 12 (1997) 805–820.
[62] W.P. Chaisson, A.C. Ravelo, Pliocene development of the east–west hydrographic gradient in the equatorial Pacific, Paleoceanography 15 (2000) 497–505.
[63] M.H. Trauth, M.A. Maslin, A. Deino, M.R. Strecker, Late Cenozoic moisture history of East Africa, Science 309 (2005) 2051–2053.
[64] P. Camberlin, S. Janicot, I. Poccard, Seasonality and atmospheric dynamics of the teleconnection between African rainfall and tropical sea-surface temperature: Atlantic vs. ENSO, Int. J. Climatol. 21 (2001) 973–1005.
[65] M. Rouault, Y. Richard, Intensity and spatial extent of drought in southern Africa, Geophys. Res. Lett. 32 (2005) L15702, doi:10.1029/2005GL022436.
[66] L. Goddard, N.E. Graham, Importance of the Indian Ocean for simulating rainfall anomalies over eastern and southern Africa, J. Geophys. Res. 104 (1999) 19099–19116.
[67] L. Bergonzini, Y. Richard, L. Petit, P. Camberlin, Zonal circulations over the Indian and Pacific Oceans and the level of lakes Victoria and Tanganyika, Int. J. Climatol. 24 (2004) 1613–1624.
[68] M.H. Trauth, A.L. Deino, A.G.N. Bergner, M.R. Strecker, East African climate change and orbital forcing during the last 175 kyr BP, Earth Planet. Sci. Lett. 206 (2003) 297–313.
[69] C.J. Luyt, J.A. Lee-Thorp, Carbon isotope ratios of Sterkfontein fossils indicate a marked shift to open environments c. 1.7 Myr ago, S. Afr. J. Sci. 99 (2003) 271–273.
[70] R. Bobe, A.K. Behrensmeyer, The expansion of grassland ecosystems in Africa in relation to mammalian evolution and the origin of the genus *Homo*, Palaeogeogr. Palaeoclimatol. Palaeoecol. 207 (2004) 399–420.
[71] T.E. Cerling, Development of grasslands and savannas in east-Africa during the Neogene, Palaeogeogr. Palaeoclimatol. Palaeoecol. 97 (1992) 241–247.
[72] N.E. Levin, J. Quade, S.W. Simpson, S. Semaw, M. Rogers, Isotopic evidence for Plio-Pleistocene environmental change at Gona, Ethiopia, Earth Planet. Sci. Lett. 219 (2004) 93–110.
[73] S.J. Feakins, P.B. deMenocal, T.I. Eglinton, Biomarker records of late Neogene changes in northeast African vegetation, Geology 33 (2005) 977–980.
[74] E.S. Vrba, On the connections between paleoclimate and evolution, in: E.S. Vrba, G.H. Denton, T.C. Partridge, L.H. Burckle (Eds.), Paleoclimate and Evolution with Emphasis on Human Origins, Yale University Press, New Haven, 1995, pp. 24–45.
[75] M.W. Wara, A.C. Ravelo, M.L. Delaney, Permanent El Nino-like conditions during the Pliocene warm period, Science 309 (2005) 758–761.
[76] K.E. Reed, Early hominid evolution and ecological change through the African Plio-Pleistocene, J. Hum. Evol. 32 (1997) 289–322.
[77] C.B. Ruff, Climate and body shape in hominid evolution, J. Hum. Evol. 21 (1991) 81–105.
[78] P.N. Gathogo, F.H. Brown, Revised stratigraphy of Area 123, Koobi Fora, Kenya, and new age estimates of its fossil mammals, including hominins, J. Hum. Evol. 51 (2006) 471–479.
[79] K. Kuman, R.J. Clarke, Stratigraphy, artefact industries and hominid associations for Sterkfontein, Member 5, J. Hum. Evol. 38 (2000) 827–847.
[80] G.P. Weedon, Time-series Analysis and Cyclostratigraphy, Cambridge University Press, Cambridge, 2003 259 pp.